Pulse distortion in GaAs quantum wells studied by a light-gating technique

Mitsuhiro Adachi and Yasuaki Masumoto
Institute of Physics, University of Tsukuba, Tsukuba, Ibaraki 305, Japan
(Received 8 March 1989)

The pulse distortion in GaAs quantum wells was studied by means of a light-gating technique. In the experiment, we used the incoherent picosecond pulse to observe accurately the changes of the coherent spike and its surrounding envelope. The experimental results clearly showed that the pulse is not anomalously delayed but is strongly distorted around the exciton resonance. We also compared the results with a computational simulation based on the absorption saturation mechanism. The simulated results agreed well with experimental results. The simulation showed that the recovery time of the exciton saturation is 90 ps around the tail part of the exciton absorption. We also observed a reduction of the coherent spike around the exciton resonance. Theoretical calculations indicate that the coherent-propagation effect in the linear absorber causes the reduction of the coherent spike.

I. INTRODUCTION

There are many interesting phenomena in the physics of pulse propagation in condensed matter. Especially associated with excitons in semiconductors, pulse distortion is expected to occur as a result of exciton-polariton effects or nonlinear-optical effects such as hole burning. In the case of bulk semiconductors, time-of-flight measurements have shown a large pulse delay due to the polariton effect.[1,2] On the other hand, in the case of two-dimensional GaAs multiple quantum wells, excitons are spatially confined in a direction perpendicular to the layers, and the wave vector normal to the layers is quantized. Therefore it is not possible to expect polariton effects in a direction perpendicular to the layers. Instead, the nonlinear-optical effect is important in excitons in semiconductor quantum wells. Hegarty investigated the phenomena, but only in a general way.[3]

In this study, we used an incoherent picosecond pulse to observe pulse propagation in GaAs quantum wells around the exciton resonance. The propagated pulses were measured by correlating with incident pulses in the nonlinear crystal. The experiment clearly demonstrates the distortion of both the pulse shape and the coherent spike. We discuss pulse distortion due to absorption saturation and reduction of the coherent spike due to the coherent-propagation effect in Secs. II and III, respectively.

II. EXPERIMENTAL PROCEDURES

The sample used in this experiment was grown by molecular-beam epitaxy (MBE) on a GaAs substrate and consists of 200 alternate periods of GaAs layers 43 Å thick and AlAs layers 62 Å thick. A window was etched in the GaAs substrate to allow passage of the laser beam. The 4-MHz laser pulses were obtained from a cavity-dumped LD700 dye laser synchronously pumped by a mode-locked Kr^+ laser. In order to generate optimum incoherent laser pulses, a real-time autocorrelator was used to monitor the laser pulses.

The weak-limit absorption spectrum of the sample at 2.1 K and three laser spectra used are shown in Fig. 1. The absorption peak in the low-energy part shows the lowest 1*s* heavy exciton, and that in the high-energy part represents a 1*s* light exciton. The absorption spectrum of the heavy exciton is centered at 1.683 eV and has an inhomogeneous linewidth of 10 meV due to fluctuations in the layer thickness. The spectral width of the laser pulses was 2.9 meV.

The schematic experimental diagram is shown in Fig. 2. The output laser beam was separated into two beams by a 50%-50% beam splitter. One beam passed through an optical delay was continuously attenuated by a neutral-density filter and was focused on the sample in the cryostat. The spot size of the laser beam on the sample surface was about 150 μm in diameter. The power density of the laser was continuously varied by the variable neutral-density filter. Another beam was bent by mirrors to be mixed with the beam propagated through

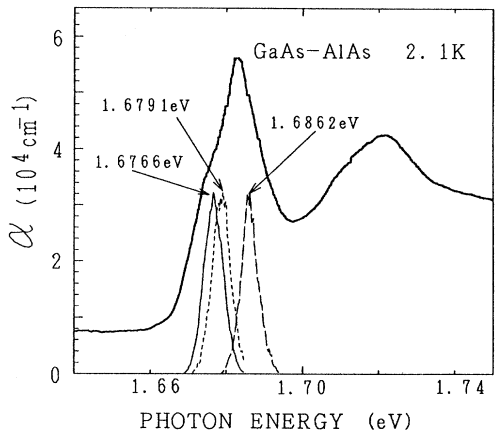

FIG. 1. Absorption spectrum of the sample and three excitation laser spectra.

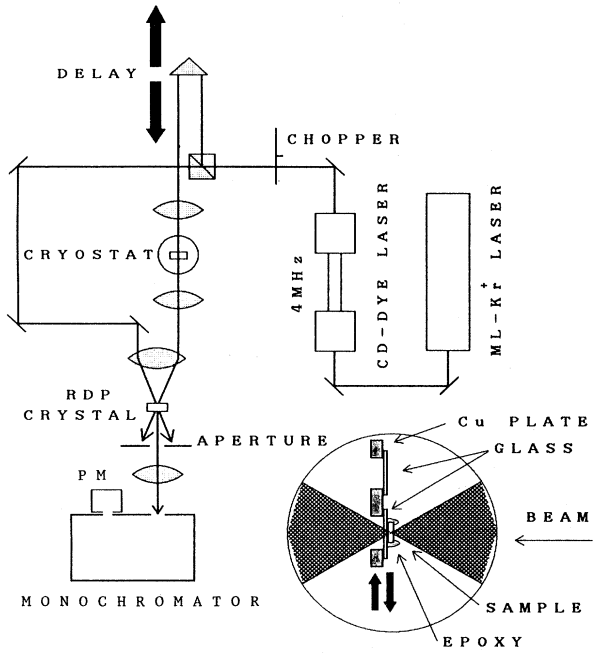

FIG. 2. Schematic diagram of experimental system. The magnified inset shows the detail of the sample surroundings.

the sample in a a rubidium dihydrogen phosphate (RDP) crystal. The correlation profile between these two beams was observed by noncollinear second-harmonic generation. The second-harmonic light was detected by a photomultiplier associated with the monochromator, whose resolution is adjusted to be 1 Å. The signal was amplified by a lock-in amplifier and processed by a computer. The optical delay was controlled with an accuracy of 10 μm by the same computer. Thus the intensity of the second-harmonic light was measured as a function of the delay time. For the purpose of measuring the coherent spike with the uppermost time resolution, we adopted an electronic micrometer (Feinprüf Millitron 1202IC and 1300) for the control of the optical delay. The computer synchronized the pulse motor to step with the output of an electronic micrometer, which can detect spatial separation down to 0.2 μm. Thus, the intensity of the coherent spike was investigated as a function of optical delay with enough time resolution and accuracy.

III. EFFECT OF ABSORPTION SATURATION

The autocorrelation traces of the laser pulse, represented by the dashed lines in Fig. 3, consist of a sharp central component, that is, a so-called coherent spike, whose correlation width is 520 fs, and a symmetrically broad correlation background envelope, whose correlation width is 19 ps. The incoherent laser pulses that give the autocorrelation traces in Fig. 3 are easily generated by adjusting a dye-laser cavity. The broad correlation envelope is close to a Lorentzian function.

The cross-correlation traces of the laser pulses, represented by solid lines in Fig. 3, consist of a broad

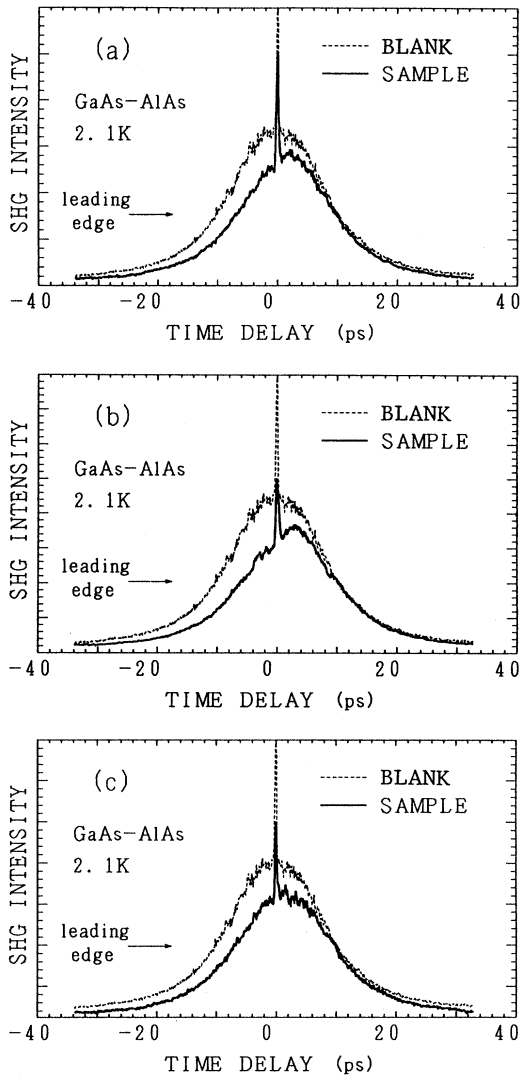

FIG. 3. SHG correlation traces. In each figure, solid lines and dashed lines correspond to cases that the sample is present or absent, respectively. The excitation power densities corresponding to (a), (b), and (c) are 2×10^{-6}, 4×10^{-7}, and 5×10^{-8} J/cm^2 pulse, respectively. Note that the cross-correlation traces are shifted by 30 fs so as to set the coherent spikes to the zero-time standard.

asymmetric correlation envelope and a coherent spike. The cross-correlation shows pulse distortion. The leading edge of the pulses was strongly absorbed, while the trailing edge was absorbed little. The pulse distortion decreases when the excitation power density decreases to $\sim10^{-8}$ J/cm^2 pulse [Fig. 3(c)] or increases to $\sim10^{-6}$ J/cm^2 pulse [Fig. 3(a)] or when the excitation photon energy increases. The pulse distortion completely disappeared when the excitation photon energy of the laser is located at the transparent energy region below the exciton resonance. These experimental results are understood in terms of the absorption saturation of exciton states in GaAs quantum wells, as described below.

The shift of the coherent spike is constant at 30 fs and

does not depend on either the excitation photon energy or the excitation power density. The shift of the coherent spike comes from the linear refractive index of the 2.1-μm-thick sample and the thin epoxy layer. This indicates that there is no detectable anomalous dispersion due to the excitons. Therefore the coherent spike is regarded as the zero-time standard so that the peak delay of the base correlation trace could be accurately decided regardless of the long-term drift. Cross-correlation traces in Fig. 3 are displayed by setting the coherent spike to the zero-time standard. Further, for the reliable determination of the peak delay, the base correlation trace was least-squares fitted by an asymmetric Lorentzian function $f(t)$:

$$f(t)=\frac{at+c}{bt^2+c} , \tag{1}$$

where a, b, and c are fitting parameters. The peak delay relative to the coherent spike is plotted in Fig. 4 as a function of the excitation power density. Note that the delay is at its maximum at a certain excitation power density. The maximum shifts towards the high excitation power density together with an increase in the excitation photon energy.

Selden has presented an equation that describes the delay of pulses propagating through a saturable absorber[4]

$$\frac{d\ln T}{dt'}+\ln T=2\beta g(t')(1-T)+\ln T_0 ,$$
$$t'=\frac{t}{\tau_s} , \tag{2}$$

where T is the transmittance at time t', T_0 is the initial transmittance at the weak-limit intensity, β is the ratio of the peak incident intensity to the saturation intensity, $g(t')$ is the normalized input pulse function, and t' is dimensionless time in units of τ_s, the relaxation time for the excited state of the absorber.

On the basis of this model, the peak shift of the correlation trace was calculated. The function of the cross-correlation traces disregarding the coherent spike $S(\tau)$ is expressed by the convolution

$$S(\tau)=\int_{-\infty}^{\infty} dt\, g(t/\tau_s-\tau)T(t/\tau_s)g(t/\tau_s) . \tag{3}$$

The temporal change of $T(t/\tau_s)$ with a certain τ_s is given by solving Eq. (2). The pulse function $g(t/\tau_s)$ used is a Lorentzian function because the convolution of Lorentzian functions is also a Lorentzian function. In Fig. 4 the calculated result for an excitation photon energy of 1.6766 eV is plotted as a function of the excitation power density as a solid line.

This calculated result is in good agreement with the experimental one when the relaxation time is $\tau_s=90$ ps. The calculations qualitatively describe the experimental feature. In particular, the calculation well describes that the delay is at its maximum at a certain excitation power density. By further calculation for 1.6791 and 1.6862 eV, the relaxation time τ_s was found to decrease together with an increase of the excitation photon energy, in agreement with a previous study.[5] The obtained relaxation times for 1.6791 and 1.6862 eV are 60 and 40 ps, respectively.

Hegarty treated the pulse delay observed in the pulse propagation in GaAs quantum wells as follows. When the pulse passes through the material, the early part of the pulse burns a hole and is strongly attenuated. The burned hole, which can be viewed as a negative absorption sitting on top of a much broader resonance, gives rise to its own anomalous dispersion, which can alter the group velocity of the remainder of the pulse. However, our experiment shows that the early part of the pulse is strongly attenuated, but there is no evidence of a pulse delay due to anomalous dispersion. Therefore, we believe that the phenomena are mostly explained by the Selden's model. There is another fault in Hegarty's model. Hegarty's model cannot explain that the peak delay attains its maximum at a certain excitation density, but Selden's model can. Nevertheless the calculated delay based on the Selden's equation is not fully consistent with the experimental one because a clear derivation is observed at a high excitation level. Selden described the saturation phenomenon as a process involving two levels. In order to improve the consistency between the experimental result and the calculated one, Eq. (2) may need to be extended to the inhomogeneously broadened excited states.

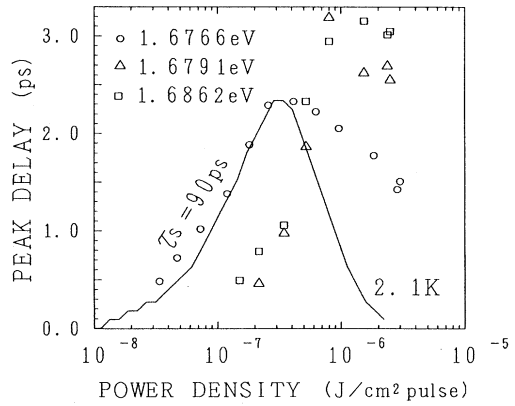

FIG. 4. Peak delay of the base correlation envelopes relative to the coherent spike as a function of the excitation power density. Experimental results are shown by symbols together with the calculated result for 1.6766 eV denoted by the solid line.

IV. COHERENT PROPAGATION EFFECT OF INCOHERENT LIGHT

The observed coherent spike showed a small but remarkable change of amplitude with a variation of the excitation photon energy. Figure 5 shows two coherent spike profiles corresponding to cases for which the sample is absent or present. Here, the base correlation trace is normalized to unity. The excitation photon energy hits the low-energy-tail part of the 1s heavy-exciton absorption. In the transparent photon-energy region, the ratio of the coherent spike to the base correlation trace does not depend on whether the sample is absent or present.

The peak amplitude ratio of the coherent spike to the

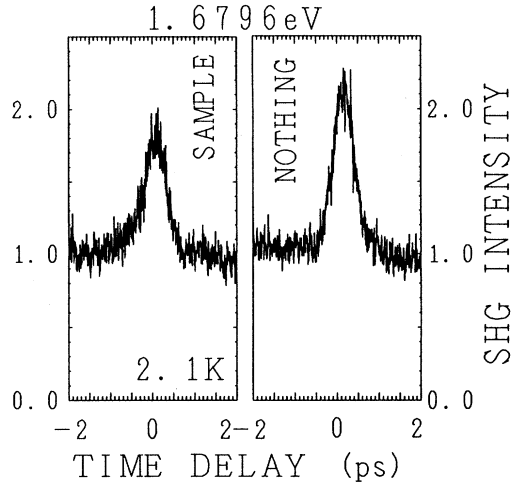

FIG. 5. The typical coherent spikes corresponding to cases that the sample is present or absent are shown. SHG intensity is normalized by the peak amplitude of the base correlation trace.

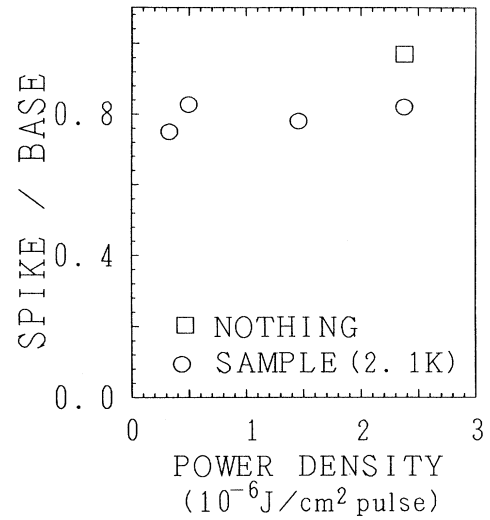

FIG. 7. The peak amplitude ratio of the coherent spike to the base correlation trace as a function of the excitation power density. The incident photon energy is 1.6796 eV.

base correlation trace is plotted in the absorption spectrum in Fig. 6. It is shown that the ratio decreases to its minimum when the incident photon energy hits the low-energy-tail part of the exciton absorption. The ratio was found to be independent of the excitation power density, as shown in Fig. 7. This means that the effect is not the nonlinear- but linear-optical effect. In order to simulate the result, a simple theoretical analysis was performed as follows.

The coherent spike is represented by a squared function of the field correlation profile

$$|\langle \tilde{E}^*(t)\tilde{E}(t+\tau)\rangle|^2 , \tag{4}$$

where $\tilde{E}(t)$ represents the amplitude of the complex light field and $\langle\ \rangle$ means the statistical average. Moreover the width of the coherent spike (520 fs) is comparable to the reciprocal of the laser spectrum width and the correlation time t_c of the field. The maximum power density used is 3.0×10^{-6} J/cm^2 pulse. This corresponds to a Rabi frequency Ω_R of 1.1×10^{10} rad/s for the $1s$ heavy exciton in the sample. We evaluated Ω_R using the relation

$$\Omega_R \equiv \frac{\mu_{1h}}{\hbar}|\tilde{E}(t)| = e\left[\frac{f_{1h}}{2m_0\hbar\omega}\right]^{1/2}|\tilde{E}(t)| ,$$

where μ_{1h} represents the electric dipole-matrix element of the $1s$ heavy exciton, $f_{1h}=1.1\times10^{-3}$ is the experimentally measured oscillation strength of the $1s$ heavy exciton,[6] e is electron charge, and m_0 is electron mass. Then $\Omega_R t_c$, which corresponds to an area of pulse during the correlation time, becomes $\pi/1000$.

Because $\tilde{E}(t)$ is incoherent, $\tilde{E}(t)$ changes its phase in random way between 0 and 2π in the duration of the correlation time t_c. Therefore it is reasonable that the optical-field envelope satisfies the following condition because the time integrals of the electric field, whose phase is randomly modulated, cancel each other:

$$\left|\frac{\mu_{1h}}{\hbar}\int_{-\infty}^{t} dt'\,\tilde{E}(t')\right| \ll 1 , \tag{5}$$

for any t. The condition (5) means that the area of a pulse is very small. Then, it is possible to apply the linear-dispersion theory developed by Crisp to the present pulse propagation phenomenon.[7] The electric-field envelope which Crisp presented is given by

$$\tilde{E}(z,t)=\frac{1}{2\pi}\int_{-\infty}^{\infty} d\omega \int_{-\infty}^{\infty} dt'\,\tilde{E}(0,t')\exp[i\omega(t'-t)] \times\exp[-\tilde{A}(\omega)z] , \tag{6}$$

where $\tilde{A}(\omega)$ and z represent the amplitude modulation factor in the medium and the propagation length in the medium, respectively. The amplitude modulation factor

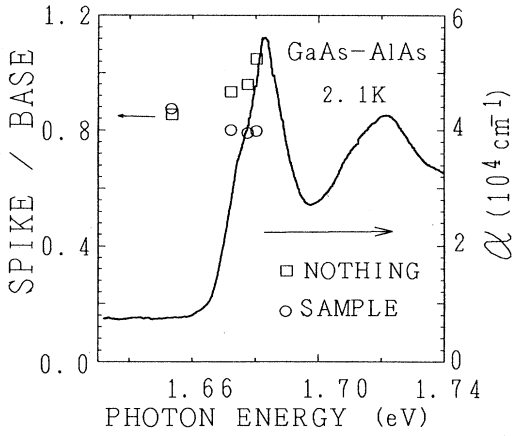

FIG. 6. The peak amplitude ratio of the coherent spike to the base correlation trace as a function of the excitation photon energy (symbols). The solid line shows the absorption spectrum.

$\tilde{A}(\omega)$ is a function of the absorption coefficient $\alpha(\omega)$ and the refractive index $n(\omega)$ of the sample as follows:

$$\tilde{A}(\omega)=\alpha(\omega)-in(\omega)\frac{\omega}{c} . \tag{7}$$

$\tilde{E}(0,t)$ means the envelope of an incident pulse at the front face of the sample. Replacing the variable $t'-t$ by s in Eq. (6), $\tilde{E}(z,t)$ is rewritten as

$$\tilde{E}(z,t)=\int_{-\infty}^{\infty} ds\, \tilde{E}(0,s+t)\tilde{F}(z,s) , \tag{8}$$

$$\tilde{F}(z,s)=\frac{1}{2\pi}\int_{-\infty}^{\infty} d\omega \exp[i\omega s-\tilde{A}(\omega)z] . \tag{9}$$

In Ref. 7, $\tilde{E}(0,t)$ was given by a short coherent pulse with small amplitude. In the present case, however, $\tilde{E}(0,t)$ is not a coherent pulse but an incoherent one. Morita *et al.* reported the calculation of incoherent pulse propagation in a study of pulse propagation in a Na-vapor cell.[8] Their calculation has an assumption as follows:

$$\tilde{E}(0,t)=V(t)R(t) , \tag{10}$$

where $R(t)$ is the Gaussian-distributed random variable of zero mean and $V(t)$ is the slowly varying envelope function. $R(t)$ in Eq. (10) reflects the characteristic feature of the coherent spike. We also adopt the same assumption. Then, the cross-correlation trace $J(\tau)$ is given by[9]

$$J(\tau)\propto\int_{-\infty}^{\infty} dt\, \tilde{E}^*(d,t)\tilde{E}(d,t)\tilde{E}^*(0,t-\tau)\tilde{E}(0,t-\tau)$$
$$\simeq\int_{-\infty}^{\infty} dt\,|V(t)|^2|V(t-\tau)|^2K(\tau) , \tag{11}$$

$$K(\tau)=\int_{-\infty}^{\infty} ds'\int_{-\infty}^{\infty} ds''\tilde{F}^*(d,s')\tilde{F}(d,s'')$$
$$\times\langle R^*(s'+t)R(s''+t)$$
$$\times R^*(t-\tau)R(t-\tau)\rangle , \tag{12}$$

where d is the sample thickness. The autocorrelation function of $R(t)$, which represents the coherent spike, is given by

$$h(\tau)=\langle R^*(t)R(t+\tau)\rangle . \tag{13}$$

It is a Fourier transform of the laser spectrum $P(\omega)$:

$$h(\tau)=\frac{1}{2\pi}\int_{-\infty}^{\infty} d\omega\, P(\omega)\exp(-i\omega\tau) . \tag{14}$$

By using Eq. (12) and the factorization property in higher-order moments of Gaussian random variables, Eq. (12) is reduced to two parts,[10]

$$K(\tau)=\left|\int_{-\infty}^{\infty} ds\,\tilde{F}(d,s)h(\tau+s)\right|^2$$
$$+\int_{-\infty}^{\infty} ds'\int_{-\infty}^{\infty} ds''\tilde{F}^*(d,s')$$
$$\times\tilde{F}(d,s'')h(s''-s')h(0) . \tag{15}$$

Another form of $K(\tau)$ is obtained by substituting Eqs. (9) and (14) into Eq. (15),

$$K(\tau)=\left[\frac{1}{2\pi}\right]^2\left|\int_{-\infty}^{\infty} d\omega\, P(\omega)\exp[-\tilde{A}(\omega)d-i\omega\tau]\right|^2$$
$$+\left[\frac{1}{2\pi}\right]^2\int_{-\infty}^{\infty} d\omega\, P(\omega)\exp\{-2\,\mathrm{Re}[\tilde{A}(\omega)]d\}$$
$$\times\int_{-\infty}^{\infty} d\omega' P(\omega') . \tag{16}$$

By substituting Eq. (7) into Eq. (6), we can obtain

$$K(\tau)=\left[\frac{1}{2\pi}\right]^2\left|\int_{-\infty}^{\infty} d\omega\, P(\omega)\exp[-\alpha(\omega)d]\cos\left[\omega\left[\tau+\frac{n(\omega)}{c}\right]\right]\right|^2$$
$$+\left[\frac{1}{2\pi}\right]^2\left|\int_{-\infty}^{\infty} d\omega\, P(\omega)\exp[-\alpha(\omega)d]\sin\left[\omega\left[\tau+\frac{n(\omega)}{c}\right]\right]\right|^2$$
$$+\left[\frac{1}{2\pi}\right]^2\int_{-\infty}^{\infty} d\omega\, P(\omega)\exp[-2\alpha(\omega)d]\int_{-\infty}^{\infty} d\omega' P(\omega') . \tag{17}$$

For the simple calculation, we assume $\alpha(\omega)$ and $n(\omega)$ as follows based on the Lorentz model:

$$\alpha(\omega)\sim\frac{4\pi\alpha_0\omega_0\Gamma/4}{(\omega_0-\omega)^2+(\Gamma/2)^2} , \tag{18}$$

$$n(\omega)\sim\frac{4\pi\alpha_0\omega_0(\omega_0-\omega)/2}{(\omega_0-\omega)^2+(\Gamma/2)^2}+1 , \tag{19}$$

where α_0 represents the exciton-phonon coupling strength. The value is adjusted to describe approximately the absorption spectrum in Fig. 1. They also satisfy Kramers-Kronig relations. Since $|V(t-\tau)|^2$ is a slowly varying function of τ compared with $K(\tau)$, $K(\tau)$ represents the coherent spike profile. The amplitude ratio of the coherent spike to the base correlation trace is obtained by comparing $K(0)$ with the wing of the $K(\tau)$ profile.

In order to clarify which dominates the reduction of the coherent spike, $n(\omega)$ or $\alpha(\omega)$, we calculated $K(\tau)$ by artificially setting one of $n(\omega)$ and $\alpha(\omega)$ to zero. Figure 8 shows the calculated ratio, corresponding to the cases of

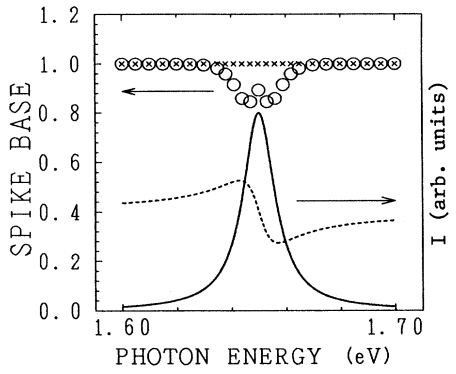

FIG. 8. The calculated result of the peak amplitude ratio of the coherent spike to the base correlation trace as a function of the excitation photon energy. Circles and crosses correspond the cases of $\{n(\omega)=0, \alpha(\omega)\neq 0\}$ and $\{n(\omega)\neq 0, \alpha(\omega)=0\}$, respectively. Here $n(\omega)$ and $\alpha(\omega)$ are the refractive index and the absorption coefficient, respectively. The solid line and the dashed line represent the model absorption spectrum and the corresponding refraction spectrum, respectively.

$\{n(\omega)=0, \alpha(\omega)\neq 0\}$ and $\{n(\omega)\neq 0, \alpha(\omega)=0\}$, when the laser spectrum $P(\omega)$ has a Gaussian profile. In the case of $\{n(\omega)\neq 0, \alpha(\omega)=0\}$, the calculated result does not show the reduction of coherent spike. On the other hand, in the case of $\{n(\omega)=0, \alpha(\omega)\neq 0\}$, it is satisfactory to account for the experimental feature in Fig. 6. The calculation clearly indicates that the absorption $\alpha(\omega)$ causes the reduction of the coherent spike but the refractive index $n(\omega)$ does not. The present work presents the first observation of the coherent-propagation effect of incoherent light in semiconductors due to the absorption $\alpha(\omega)$.

V. CONCLUSIONS

A remarkable pulse distortion in GaAs quantum wells was observed around the exciton resonance by means of a light-gating technique. We demonstrated the usefulness of incoherent pulses in observing the distortion of both the pulse envelope and the coherent spike. The pulse was strongly distorted, but was not anomalously delayed. The pulse distortion in GaAs quantum wells around the exciton resonance is well understood by taking account of the absorption saturation. The relaxation time $\tau_s = 90$ ps obtained by our experiments is comparable to the result of a pump and probe experiment previously presented. The second-harmonic generation (SHG) cross-correlation technique is a conventional technique used to study the ultrafast temporal change of absorption saturation under certain conditions. The reduction of the coherent spike observed experimentally was explained by taking account of the coherent-propagation effect in the linear absorber. The effect was observed in semiconductors for the first time in the present experiment.

ACKNOWLEDGMENTS

The authors wish to thank Dr. M. Tanaka at the National Research Laboratory of Metrology for the useful technical advice on time-resolved measurements with high precision. This work was in part supported by Grant-in-Aid No. 63604511 for Scientific Research on Priority Areas, New Functionality Materials–Design, Preparation, and Control–by the Ministry of Education, Science and Culture of Japan.

[1]Y. Masumoto, Y. Unuma, Y. Tanaka, and S. Shionoya, J. Phys. Soc. Jpn. **47**, 1844 (1979).
[2]R. G. Ulbrich and G. W. Fehrenbach, Phys. Rev. Lett. **43**, 963 (1979).
[3]J. Hegarty, Phys. Rev. B **25**, 4324 (1982).
[4]A. C. Selden, J. Phys. D **3**, 1935 (1970).
[5]J. Hegarty and M. D. Sturge, J. Opt. Soc. Am. **B2**, 1143 (1985).
[6]Y. Masumoto, M. Matsuura, S. Tarucha, and H. Okamoto, Phys. Rev. B **32**, 4725 (1985).
[7]M. D. Crisp, Phys. Rev. A **1**, 1604 (1970).
[8]N. Morita, K. Torizuka, and T. Yajima, J. Opt. Soc. Am. **B3** 548 (1986).
[9]E. P. Ippen and C. V. Shank, in *Ultrashort Light Pulses,* edited by S. L. Shapiro (Springer, New York, 1977), Chap. 3.
[10]R Loudon, *The Quantum Theory of Light* (Oxford University Press, Oxford, 1978), Chap. 5.